Reports

A Large-Scale Hole in the Ionosphere Caused by the Launch of Skylab

Abstract. *A dramatic ionospheric phenomenon, unique in magnitude and in spatial and temporal extent, occurred along the Atlantic Coast of North America after the launch of the NASA Skylab Workshop on 14 May 1973. The effect was a large and rapid decrease in the total number of ionospheric electrons within a distance of 1000 kilometers of the burning engines of the Saturn V launch vehicle. The observations are interpreted in terms of exceptionally enhanced chemical loss rates due to the molecular hydrogen and water vapor contained in the Saturn second-stage exhaust plume.*

A very-high-frequency radio signal passing through the earth's ionosphere experiences a continual rotation of its plane of polarization due to the presence of many low-energy electrons and the geomagnetic field. This "Faraday rotation effect" may be used to infer valuable information about the electron content of the ionosphere. If $N_e(h)$ denotes the concentration of electrons N_e as a function of height h, then the integral of $N_e(h)$ with height is called the ionospheric total electron content (TEC). It is a measure of the total number of electrons in a vertical column of unit cross section through the ionosphere. For experiments involving the use of a geostationary satellite's very-high-frequency radio beacon, the polarization observations yield the number of ionospheric electrons contained in a vertical column extending to approximately 2000 km (*1*).

Continuous observations of the TEC have been made at the Sagamore Hill Radio Observatory (*2*) in Hamilton, Massachusetts, since November 1967. At approximately 12:39 E.S.T. on 14 May 1973, a sudden decrease in the TEC was observed along the ray path to the geostationary telecommunication satellite ATS-3. Figure 1A is a plot of the 15-minute TEC values (in units of 10^{12} electron/cm^2) as a function of time (E.S.T.) for that date. The solid curve in Fig. 1B gives an expanded version of the TEC decrease, whereas the curves with dots and crosses give theoretical results to be discussed below. Between 12:30 and 12:45 E.S.T. the TEC dropped from 11.3 to 5.8 units. The value was below 5 units from 13:00 to 14:00 E.S.T., and then slowly began to recover. The dashed diurnal curve in Fig. 1A gives an estimate of the expected behavior for the TEC on the day in question. This curve incorporates the predicted monthly mean TEC for May 1973, corrected for the effects of geomagnetic activity (*3*). The large "bite-out" seen in the TEC data for 14 May clearly distinguishes itself from the expected behavior for that day. Ionospheric disturbances monitored in terms of the TEC values at Sagamore Hill have been extensively studied for many years (*4*); it can be stated with confidence that this sudden and large drop in the daytime TEC is a unique disturbance unrelated to any solar or geomagnetic activity. The aim of this report is to point out the geographical and temporal extent of this effect and to suggest as its cause an exceptionally enhanced electron loss mechanism in the upper atmosphere triggered by the launch of the NASA Skylab Workshop (Skylab 1).

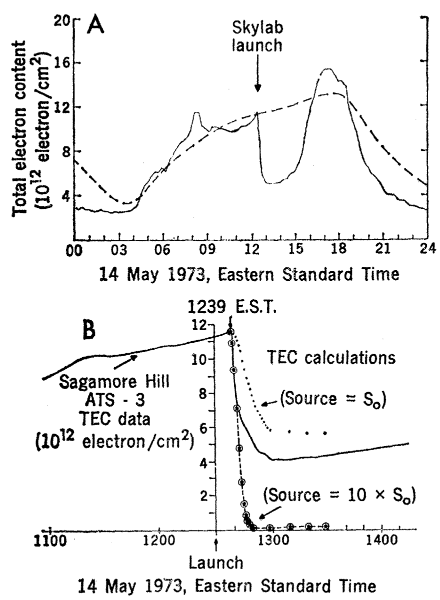

Fig. 1. (A) The solid curve shows the ionospheric TEC as a function of time (E.S.T.) on 14 May 1973, as observed at the AFCRL's Sagamore Hill Radio Observatory in Hamilton, Massachusetts. The dashed curve gives the expected behavior for that day, and the vertical arrow marks the time of the Skylab launch at 12:30 E.S.T. from the Kennedy Space Center. (B) Expanded version of the TEC decay showing the results of continuity equation estimates of the time development of the TEC. The dots refer to results obtained using the enhanced loss rates which result from 1 second of exhaust, and the crosses give the results for 10 seconds of exhaust.

Skylab 1 was launched at 12:30 E.S.T. on 14 May 1973 from pad A, complex 39 (28.4°N, 80.6°W), at the Kennedy Space Center, Cape Canaveral, Florida. A comparison of the Saturn/Skylab trajectory (*5*) and the Faraday rotation propagation geometry showed that the vehicle crossed the vertical plane defined by the Sagamore Hill ray path to ATS-3 at 36.8°N, 74.7°W, and a height of 422 km. The satellite ray passed 208 km above this point at 630 km; the horizontal separation of the trajectory from the ray path was approximately 210 km, and thus the point of closest approach was about 150 km.

The Saturn V launch vehicle consisted of two stages. The first stage (S-I), burning kerosene in an O_2 environment, cut off at 88 km and therefore was of little interest for the possible F-region effects to be considered here. The second stage (S-II) consisted of a cluster of five J-2 engines burning H_2 in an O_2 environment. All five of the J-2 engines ignited at a height of 88 km; the center engine then cut off at 273 km, and the remaining four continued to burn until orbit in-

Scoreboard for Reports: In the past few weeks the editors have received an average of 63 Reports per week and have accepted 11 (17 percent). We plan to accept about 10 reports per week for the next several weeks. In the selection of papers to be published we must deal with several factors: the number of good papers submitted, the number of accepted papers that have not yet been published, the balance of subjects, and length of individual papers.

Authors of Reports published in *Science* find that their results receive good attention from an interdisciplinary audience. Most contributors send us excellent papers that meet high scientific standards. We seek to publish papers on a wide range of subjects, but financial limitations restrict the number of Reports published to about 12 per week. Certain fields are overrepresented. In order to achieve better balance of content, the acceptance rate of items dealing with physical science will be greater than average.

sertion at 442 km. Each engine had a thrust of 239,000 pounds of force (108,000 kg of force) which it achieved by ejecting mass at the rate of 537 pounds of mass per second at a speed of 15,000 feet/sec (4500 m/sec). The exhaust was composed of 70 percent water vapor and 30 percent unused H_2 (*6*). When converted to particle flow per second, each J-2 engine ejected 7.8×10^{27} H_2O molecules per second and 3.3×10^{27} H_2 molecules per second at a speed of 4.5 km/sec. Such flow rates represent extraordinary additions to the ambient atmosphere, and of species never found in quantity in the ionospheric F region. With the cluster of engines releasing over a ton per second of such gases, one might expect to find a variety of dynamical and chemical processes of direct ionospheric consequence.

Under normal conditions, the ionospheric F region is produced by the photoionization of atomic oxygen by solar radiation at extreme ultraviolet and soft x-ray wavelengths. Equal numbers of electrons (e^-) and positive ions (O^+) are produced in a ratio to neutral oxygen (O) of approximately 1:1000. The loss (or recombination) mechanism for the O^+ and e^- is a well-understood process (*7*) involving intermediate reactions with N_2 and O_2. When the Saturn V engines added large numbers of H_2 and water vapor molecules to the F region, the normal ionospheric chemistry was substantially altered. Specifically, the constituents of the Saturn exhaust initiated a recombination process between the ionospheric O^+ and the ambient electrons. The overall mechanism was a two-step process involving first the formation by O^+ of a molecular ion and then a dissociative recombination of that ion with one of the F-region electrons. The end result of the two reactions was thus the removal of an ionospheric ion-electron pair.

The first step in the loss process initiated by the Saturn exhaust (*8*) was

$$O^+ + H_2 \rightarrow OH^+ + H \quad (1)$$

or

$$O^+ + H_2O \rightarrow H_2O^+ + O \quad (2)$$

The second step was

$$OH^+ + e^- \rightarrow O + H \quad (3)$$

or

$$H_2O^+ + e^- \rightarrow H_2 + O \quad (4)$$

or

$$H_2O^+ + e^- \rightarrow OH + H \quad (5)$$

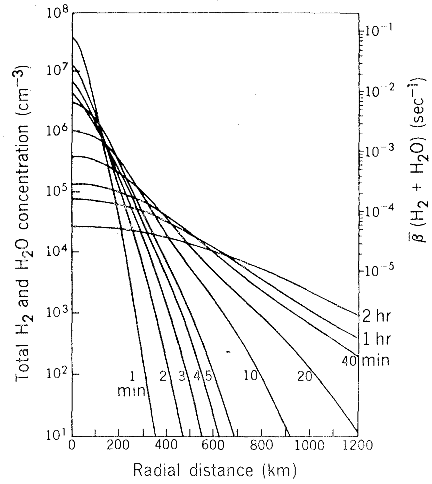

Fig. 2. Results of spherical diffusion model calculations for H_2 and H_2O in the ionosphere. Each curve gives the total plume concentration as a function of radial distance for a series of elapsed times. The source at the origin was defined to be the number of molecules ejected by the Saturn engines in 1 second. The axis on the right gives the average electron loss coefficient ($\bar{\beta}$). The calculations were carried out with the use of atmospheric variables defined at 350 km (see text).

The remarkable feature about Eqs. 1 and 2 is that they proceed at the kinetic rate, that is, a reaction occurs with virtually every ion-molecule collision. This is drastically different from the normal ionospheric case in which O^+ reacts with N_2 and O_2. The reactions of O^+ with H_2 and water vapor are more rapid, by a factor of 100 to 1000 times, than the reactions of O^+ with N_2 and O_2, and thus the formation of positive molecular ions via Eqs. 1 and 2 is an abnormally fast one for the F2 region. Once a molecular ion is formed (whether OH^+, H_2O^+, NO^+, or O_2^+), the subsequent dissociative recombination reactions are all of the form of Eqs. 3, 4, or 5. Such reactions are rapid and provide the principal mechanism of ion-electron recombination in the ionosphere (*9*). Since the overall loss mechanism involves two steps, the actual loss rate for electrons depends ultimately upon the speed of the slower ion-atom interchange reactions. Since the reactions of H_2 and H_2O with O^+ are approximately 1000 times faster than normal, concentrations of H_2 or H_2O, or both, only 0.1 the ambient N_2 concentration will produce a 100-fold enhancement in the electron loss rates. If one measures the rate of change of the TEC during the period immediately after the Skylab launch (Fig. 1), one sees that the observed electron loss rate is in fact greater than normal by a factor of 100 to 200 times (*10*).

The above examination of reaction rates, together with the realization that a ton of reactant is added to the ionosphere every second by the Saturn engines, leads to the conclusion that the electrons throughout the topside F region experienced a devastating loss process in the vicinity of the S-II plume. Consider, for example, that during the 275-second interval from the time of the S-II center engine cutoff (at 273 km) to engine shutdown (at 442 km), the four J-2 engines released a combined total of 1.2×10^{31} H_2 and H_2O molecules. At a height of 350 km, a plume concentration of these molecules of 2×10^6 cm^{-3} would cause the electron loss rates due to H_2 and H_2O to become 100 times more efficient than the normally dominant loss mechanism. The 275-second exhaust from the four J-2 engines gives such a concentration if uniformly distributed throughout a volume of about 6×10^{24} cm^3. This implies that the scale size for dramatic ionospheric effects should be of order (volume)$^{1/3}$ or about 1800 km. An examination of the TEC data from sites in Goose Bay, Labrador, and Urbana, Illinois, showed that a definite decrease in the TEC was indeed observed at points 1000 km to the north and west of the trajectory of the burning Saturn rocket in the F region. These and other (more detailed) aspects of this study are described elsewhere (*3*).

In the effects described so far we have dealt only with the reactions made possible by the constituents of the exhaust field of the Saturn launch vehicle. Clearly, the dynamics of the plume must also be considered if the temporal and spatial aspects of the problem are to be compared with observations. As a way of doing this, we now consider a model of spherically symmetrical diffusion of the plume in the ionosphere. We anticipate that such a model will overestimate diffusion in the downward direction, underestimate it in the upward direction, and therefore give a reasonable overall view of the gross effects to be expected as a function of distance and time. We treat the H_2 and water vapor components separately and take as point sources for the model the total number of H_2 or H_2O molecules ejected by the engines in 1 second. We choose as the second in question the instant when the vehicle was at 350 km. At this time, the speed of the vehicle with respect to the atmosphere equaled the speed of the exhaust with respect to the vehicle, and thus the exhaust entered the ionosphere at a relative speed of zero. During the 1-second interval used, the rocket moved 4.5 km while emitting a total of 1.32×10^{28} H_2 molecules and 3.12×10^{28} H_2O molecules. A standard solution (*11*) of the radial diffusion equation is

$$n(r,t) = \frac{S_0}{(4\pi Dt)^{3/2}} \exp(-r^2/4Dt) \quad (6)$$

where, for each species, n is the concentration at a radial distance r and time t, S_0 is the total number of particles at $r = 0$ and $t = 0$, and D is the diffusion coefficient in an oxygen (O) atmosphere. Using Eq. 6, we carried out calculations to a distance of 1200 km for a time span of 2 hours. The total plume concentration was obtained by adding the contributions from each expending cloud; the results that are shown in Fig. 2 lead to several interesting findings:

1) The plume diffuses so rapidly that within a few minutes the loss coefficient throughout a volume of several hundred kilometers radius is larger than the normal loss rates by a factor of 10 to 100 times.

2) Although the exhaust field is H_2O-dominated in terms of total concentrations, the onset of the TEC "biteout" was determined by the arrival of the H_2. This is due to the fact that the lighter constituent diffuses more rapidly. The duration of the effect, however, is due mainly to the more slowly diffusing water vapor.

3) At a given radial distance from the source, there is a unique time when maximum H_2 and H_2O and total concentrations occur (*12*). For example, at a distance of 200 km, the maximum H_2 concentration occurs after 3 minutes of expansion, whereas at 600 km it occurs 27 minutes after the source is released. Thus, a chain of stations would record maximum effects sequentially. It is as if a wave passed along the chain, though it must be noted that for each species the concentration is always a maximum at $r = 0$ for any given time.

Calculations were also carried out which show that, during the time interval under consideration here, the plume could not have suffered any appreciable depletions due to solar-induced photoionizations or dissociations (*3*).

The actual loss in electron content to be expected from the plume can be calculated using the loss coefficients obtained from the H_2 and H_2O results summarized in Fig. 2. If the TEC data are considered to represent the integral of a slab of plasma located 200 km from the source, the TEC response may be explicitly evaluated as a function of time (*13*). This calculation was carried out at 1-minute intervals for a duration of 20 minutes, and then at 10-minute steps up to an hour. The results are compared with observations in Fig. 1B. The dotted curve gives the results of the TEC calculations in which the H_2 and H_2O loss coefficients which result from 1 second of exhaust (S_0) are used. The calculations clearly lead to a relatively rapid drop in the TEC. After about 20 minutes, the slowly decaying H_2 and H_2O concentrations cause the total loss to equal the solar production effects and thus the TEC remains nearly constant.

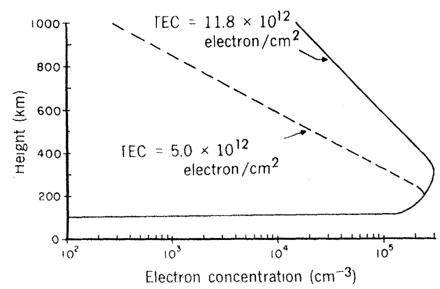

Fig. 3. Representative $N_e(h)$ profiles that yield the TEC values observed at Sagamore Hill before and after the Skylab launch.

The second set of results presented in Fig. 1B describes calculations derived from the use of a point source equal to the total number of particles ejected in 10 seconds. During this time interval the vehicle moved only 45 km, a distance comparable to the mean free path and still small in comparison to the 200-km distance under consideration. These results are in excellent agreement with the onset of the decay, but the calculations subsequently predict a virtual disappearance of the electron content. We suggest that this vanishing of the TEC is indeed what happened to the topside content of the F2 region. The plateau of "minimum of the biteout" in our observations near 5×10^{12} electron/cm^2 simply represents the contributions of the bottomside ionospheric regions (E, F1) to the TEC integral.

Figure 3 presents a schematic representation of two possible electron density profiles which, when integrated up to 1000 km, equal the TEC values measured prior to and during the "Skylab bite-out." These profiles were obtained from ionosonde values of the critical frequencies of the E, F1, and F2 regions (as observed from Wallops Island, Virginia), coupled to ionospheric models for the shape of the topside. Above the peak in the ionosphere, reductions occur of up to 10^{-2} of the prelaunch values.

Although rockets of various types have been launched into the ionosphere and perturbations have been caused by them, no effects remotely approaching the extent of the present case have ever been reported. The 12 Saturn V rockets launched during the Apollo program did not cause similar ionospheric holes because all of their final parking orbits (and therefore their second-stage burns) were below 190 km where the ionospheric chemistry is of a different type from the F-region processes affected by the Skylab launch (orbit insertion at 442 km).

In conclusion, it is interesting to consider that this significant recombination effect in the ionosphere was apparently unanticipated. Hydrogen, the most abundant element in the universe, is not normally found in molecular form in significant quantities in the near-earth environment. It is, however, an important constituent in interstellar space, and thus the fast reaction between H_2 and O^+ has interesting implications in astrophysics. There is also the potential for important geophysical modification experiments. Concerning this point, H_2 has the asset of being light and particularly resistant to a quick destruction by solar extreme ultraviolet, whereas water vapor has the interesting property that the dissociative recombination of H_2O^+ yields a product (either H_2 or OH) capable of engaging in another O^+ ion-atom interchange reaction. Thus, the net effect is that a single H_2O molecule would remove two F-region ion-electron pairs. Although the O^+ reaction with the OH radical has not been measured in the laboratory, its rate is expected to be close to that of H_2 and H_2O (*14*). Again, OH is a prominent interstellar constituent.

MICHAEL MENDILLO
Department of Astronomy, Boston University, Boston, Massachusetts 02215

GERALD S. HAWKINS
Smithsonian Astrophysical Observatory, Cambridge, Massachusetts 02138

JOHN A. KLOBUCHAR
Air Force Cambridge Research Laboratories, Bedford, Massachusetts 01730

References and Notes

1. J. E. Titheridge, *Planet. Space Sci.* **20**, 353 (1972).
2. Operated by the Air Force Cambridge Research Laboratories (AFCRL), Hanscom Air Force Base, Bedford, Massachusetts.
3. M. Mendillo, G. S. Hawkins, J. A. Klobuchar, *Tech. Rep. TR-74-0342, ERP 483* (Air Force Cambridge Research Laboratories, Hanscom Air Force Base, Bedford, Massachusetts, July 1974).
4. M. Mendillo and J. A. Klobuchar, *Tech. Rep. TR-74-0065* (Air Force Cambridge Research Laboratories, Hanscom Air Force Base, Bedford, Massachusetts, 1974).
5. G. T. Pinson, *Tech. Rep. D5-15560-13* (Boeing Company, Huntsville, Alabama, 1973).
6. S. A. Sadunas, E. P. French, H. Seaton, *NASA Contractor Rep. 129009* (Rockwell International Corporation, Downey, California, 1973).
7. H. Rishbeth and O. K. Garriott, *Introduction to Ionospheric Physics* (Academic Press, New York, 1969), chap. 3.
8. E. E. Ferguson, *Atomic Data Nuclear Data Tables* **12**, 159 (1973). Ferguson quotes as rate constants for Eqs. 1 and 2, respectively, 2.0×10^{-9} cm³/sec and 2.4×10^{-9} cm³/sec, $\pm$ 30 percent.
9. P. M. Banks and G. Kockarts [*Aeronomy* (Academic Press, New York, 1973), part A, chap. 10] point out that the dissociative recombination rate constants are of the order of 10^{-7} cm³/sec.
10. The loss of the TEC is usually described by

$$\frac{d\,\mathrm{TEC}}{dt} = -\beta_{\mathrm{eff}}\,\mathrm{TEC}$$

where the effective loss coefficient (β_{eff}) is typically equal to 2×10^{-5} to 4×10^{-5} sec^{-1}. It is determined from theory, or from observations after sunset when solar production ceases and the TEC slowly decays to low nighttime values.
11. W. Jost, *Diffusion* (Academic Press, New York, 1960), chap. 1.
12. The exact relationship

$$t_{\mathrm{max}} = \frac{1}{6}\frac{r^2}{D}$$

is obtained by setting the time derivative of Eq. 6 equal to zero. For H_2, it numerically becomes $t_{\mathrm{max}} \approx 3/4\ r^2$, where t_{max} is in minutes and r is in hundreds of kilometers.
13. In the more rigorous treatment (*3*), the TEC is evaluated using

$$d\mathrm{TEC}(t)/dt = Q - [\beta_{\mathrm{eff}} + \beta_{\mathrm{H_2}}(t) + \beta_{\mathrm{H_2O}}(t)]\ \mathrm{TEC}(t)$$

where Q is a modified production function obtained from the average rate of change of TEC prior to the launch.
14. E. E. Ferguson, personal communication.
15. We thank Dr. J. Aarons of the Ionospheric Physics Laboratory (AFCRL) for his encouragement and support. We thank Dr. W. Swider (AFCRL) who provided valuable assistance concerning the aeronomic processes involved in this study, and S. Sadunas (Rockwell International, Downey, California) and C. Varnardo (NASA, Huntsville, Alabama) who kindly furnished the answers to various technical questions concerning Saturn V launches. M.M. was supported under a National Research Council–National Academy of Sciences resident research associateship at AFCRL (1972–1974). G.S.H. is currently at AFCRL as senior resident research associate with the support of the National Research Council–National Academy of Sciences, on leave from the Smithsonian Astrophysical Observatory.

16 September 1974; revised 25 October 1974 ■

Seasonal Change of Antarctic Sea Ice Cover

Abstract. *The winter expansion of the sea ice surrounding Antarctica and the subsequent retreat of the ice in summer may be linked with the wind stress acting on the Southern Ocean in conjunction with the heat exchange in open water regions within the ice fields.*

The Antarctic sea ice undergoes immense seasonal fluctuations in areal extent (Fig. 1). The maximum area, 22×10^6 km², occurs in September and the minimum, 4×10^6 km², in March (*1*). Although other estimates differ slightly (*2, 3*), all indicate seasonal variations of approximately 18×10^6 km², an area larger than that of Antarctica and its ice shelves.

Sea ice acts as an insulator, effectively reducing radiative and nonradiative heat flux between ocean and atmosphere (*4*). In summer, when incoming solar radiation is large, the ice reflects 40 to 70 percent of this radiation to drastically reduce heating of the ocean; if the ocean were ice-free it would reflect only 10 percent (*4*). In winter the ice cuts down substantially on the sensible and latent heat flux from ocean to atmosphere, because of its low heat conductivity and low vapor pressure (*4*).

Sea ice, with a salinity of 3 to 5 per mil (*5*), is an important factor in the ocean's salt balance, ejecting some 3 g of salt per square centimeter of surface as a cold brine into the ocean for each meter of ice formed. This process reduces the stability of the ocean surface layer and convection can ensue. The convection may penetrate the relatively warm-saline upper layers of circumpolar deep water (400 to 600 m deep), which would result in a significant upward heat flux into the surface layers and eventually into the atmosphere (*6, 7*). During ice melting the release of relatively fresh water increases the stability of the surface layer, retarding convection.

Hence, the seasonal variation of the ice has important effects on the thermohaline structure of the ocean and on the characteristics of the atmosphere. The reason for the large seasonal change has not been investigated; presumably new ice is added in winter to the outer fringes of the sea ice field and removed the following summer. We present the hypothesis that much of the ice growth and retreat is due to processes related to the wind stress within the sea ice fields.

The curl of the wind stress (*8*), which induces a general Ekman divergence of surface water and sea ice cover, continuously generates open water regions with freezing point temperatures within the ice fields. In winter the open water fills with new ice and the ice field expands accordingly, extending northward as a function of the total divergence within the existing ice field. The northern extent of the ice may be determined by an inability of the local heat balance (in both atmosphere and ocean) to continually freeze over the open water generated by the Ekman divergence. The resulting partial ice cover may then be destroyed by ocean waves which penetrate into the ice field. After the spring equinox, open water regions within the ice field increase heat absorption by the ocean, and rapid ice melting follows.

The hypothesis can be evaluated by comparing the observed winter growth rate of the ice with the rate calculated from the Ekman divergence. Figure 1 indicates an observed growth rate (mid-March to mid-August) of 3.3×10^6 km² per month.

The rate of divergence of the ice can only be estimated, since understanding of the behavior of ice on a boundary layer is incomplete, although one would anticipate less interference of ice with the ocean-atmosphere coupling in a divergent Ekman field (*9*). In view of these uncertainties we cannot firmly establish the validity of our hypothesis. However, we can test to see if it is reasonable.

The total Ekman transport is directed at a right angle to the surface wind direction and is proportional to the ratio of wind stress to Coriolis parameter (*10*). However, the full magnitude of the drift is accounted for in the upper half of the Ekman layer, and is directed 78° to the left of the wind direction in the Southern Hemisphere. Below this segment of the Ekman layer the contribution to the total drift vector is a further 12° rotation to the left of the wind direction. Therefore, the total divergence is calculated by assuming uniform horizontal flow in the upper half of the Ekman layer. The Ekman is taken to be equivalent to the thickness of the mixed layer (*11*), which in the ice field is about 40 m (*7*). The data in